DYNAMIC KINKING OF A CRACK IN PLANE STRAIN

P. BURGERS†

Department of Mechanical Engineering and Applied Mechanics, 111 Towne Bldg./D3, University of Pennsylvania, Philadelphia, PA 19104, U.S.A.

Abstract—The kinking of an initially stationary crack in a linear elastic body due to dynamic loading is solved using linear superposition to construct dual singular integral equations, which are solved numerically. The results for stress wave loading as well as loading on the crack faces only are presented, with an estimated accuracy of better than 3%. Some conclusions on crack velocity and kink angle are drawn for a fracture criterion which requires $K_{II} = 0$.

INTRODUCTION

When dynamic loading is applied to a body with internal cracks, the resulting stress wave may cause the stress intensity factor at any crack tip to become greater than the value required for initiation of crack growth and continued crack propagation. The direction of propagation, as well as the velocity of crack propagation, at the instant of initiation will depend on the local stress field around the crack tip. These situations are of importance in many problems: for example, earthquake generated stress waves impinging on faults in the mantle of the earth, explosive mining of coal by rubblerizing material underground and the extension of fractures to improve the permeability of oil bearing rock around a borehole for better recovery of oil.

It is only recently that experiments have been performed carefully enough that they can be modeled mathematically. In particular, the experiments of Ravi-Chander and Knauss[1] appear to be close to producing the required information for determining precisely the criterion for crack kinking due to stress wave loading. The experiments are obviously difficult to do and it is important that they be interpreted correctly.

The analysis undertaken here is the extension of previous work[2] in which a crack subjected to an anti-plane strain stress wave loading (and other loadings) was solved. For this case, verification of the accuracy of the numerical method was made by comparing the results with analytical results presented in Burgers and Dempsey[3]. The numerical method for the plane strain case considered here, is very similar to that used in the Mode III case. Analytical results in plane strain are so far limited to the case when no kinking occurs. The numerical results for the straight crack case are of the same accuracy as for the Mode III problem. Using this fact and that the method follows that used to analyze the Mode III case, it is believed that the results for all kinking angles considered in the plane strain case will be of the same accuracy as the results in [3]; that is within 3% of the correct results.

The analysis requires that the problem considered be self-similar in the variables r and t, where r is the radial distance from the origin and t is time. This puts a restriction on the problems that can be considered. However, it is felt that the solutions obtained below will give some insight into the kinking of a crack and how the analysis can be extended to the physically correct problem.

The kinking of a crack in plane strain has also been considered in [4] where the problem was solved by finite differences. Due to the difficulty in interpolation of singular stress fields near the kink and the crack tip, the results in [4] are not thought to be accurate for short times after kinking, although they may improve for longer times. The method in [4] is however more generally applicable than that used here and problems which are not self-similar in r and t can be treated.

THE KINKED CRACK: PROBLEM DEFINITION AND METHOD OF SOLUTION

We require that the problems considered be self-similar in the variables r and t. For this paper we will consider only the case when stresses are functions of r/t. For this to be so, the geometry must have no characteristic length associated with it.

†Present address: Hibbitt, Karlsson and Sorensen, Inc., 35 South Angell St., Providence, RI 02906, U.S.A.
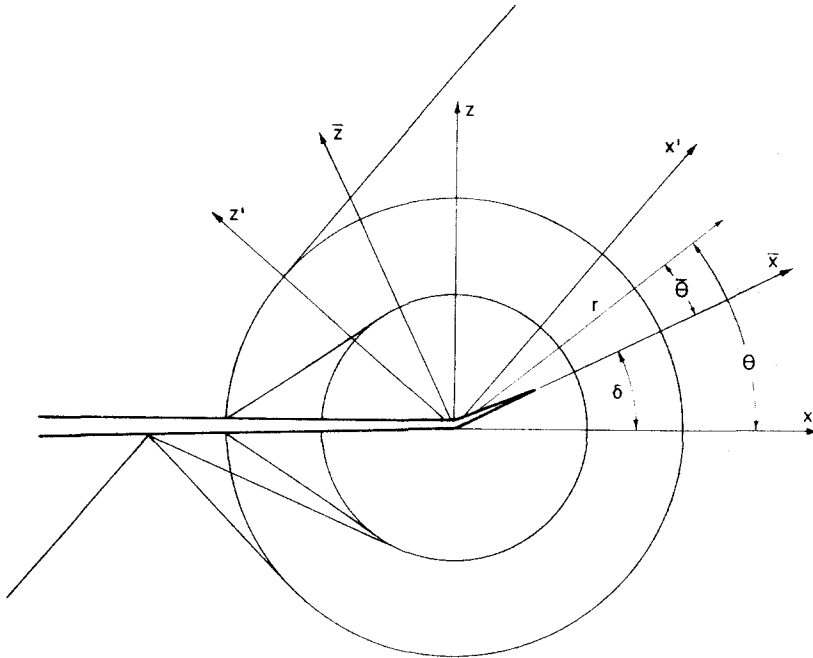
Fig. 1. Stress wavefront pattern for a planar normal stress-wave impacting a semi-infinite crack.

The geometry for the kinked crack under consideration with the wavefront pattern for planar normal stress wave loading is shown in Fig. 1. In a stress-free linear elastic homogenous isotropic full-space there exists a stationary semi-infinite crack, which will be referred to as the old crack. At time $t = 0$, a crack, referred to as the new crack, propagates out of the tip of the semi-infinite crack. The velocity of propagation v_{CT} is constant, and the line of propagation is straight, making an angle δ with the semi-infinite crack. Also, at time $t = 0$ some loading is applied. As already stated, this loading must generate stresses which are self-similar in r and t. Examples of this type of loading are; case (a) constant tractions appearing on the faces of the new crack; case (b) tractions applied to the old crack faces as a step function in time and of constant magnitude in space; and case (c) a planar stress wave of constant magnitude, making an angle α with the old crack line and reaching the origin of time $t = 0$. Note that for the case when $\alpha = 0$, the loading cases (a) and (b) can be combined (after multiplication by the correct constants) to give case (c).

We follow the method using superposition of dislocations described in [2, 5]. This method was initially used to solve static fracture problems; see the article by Rice[6] for a review of applications and theory. We start by solving the problem of a dislocation being emitted from the tip of the old crack along the line $\theta = \delta$. Since the skew crack problem is not symmetric about the line $\theta = \delta$, it involves both Mode I and Mode II deformation and the two cases of an edge dislocation (where the Burgers vector is a displacement discontinuity perpendicular to the dislocation path) and a shear dislocation (where the Burgers vector is a displacement discontinuity parallel to the dislocation path) are required. The dislocations propagate out from the tip of the old crack at constant velocity u. This velocity will be used as the superposition parameter; that is a distribution of dislocations with velocities u varying from zero to v_{CT} will be used. For the problems considered, the resultant stress distribution due to this superposition must be self-similar and this implies that the form of the discontinuity of each dislocation must generate self-similar stresses; that is, the Burgers vector must grow linearly with time.

When these dislocation solutions are superimposed using as yet unknown distributions for the edge and shear dislocations, the resultant stress along the crack line can be equated to some known function; for example, equal to the magnitude of the applied traction components on the new crack faces for loading case (a). This results in a Cauchy singular

integral equation for which there are a number of very accurate numerical methods[2, 7–9], which can be used to obtain the stress intensity factors. To obtain the dislocation solutions, a number of simpler problems are used. These solutions are obtained in terms of definite integrals which must be evaluated numerically.

REQUIRED GREEN'S FUNCTION SOLUTIONS

Edge dislocation growing linearly with time

Consider an edge dislocation which appears in a linear elastic full-space at time $t = 0$ (with no crack). The -ve x-axis lines up with the old crack line, with the origin at the old crack tip. The $\bar{x}$-axis lines up with the new crack line, making an angle δ with the x-axis. See Fig. 2(a). One end of the dislocation propagates out along the $\bar{x}$-axis at a constant velocity w and the other end remains stationary at the origin, $\bar{x} = 0$. The Burgers vector grows linearly with time as discussed above.

The displacements are given by u_x, u_z in the x, z directions, respectively. By the plane strain assumption, $u_y \equiv 0$. The relevant stress components needed for solving the boundary value problem are σ_{xx}, σ_{xz} and σ_{zz}. A bar over a superscript will indicate if a quantity is represented in the $\bar{x}$-$\bar{z}$ coordinate system, e.g. $u_{\bar{z}}$ is the displacement in the $\bar{z}$-direction.

The full space is considered to be at rest for all $t \leq 0$ with zero displacements; that is, zero initial conditions only are considered. (This applies to all subsequent problems as well.) From symmetry we note that only the half-plane $\bar{z} = 0$ need be considered. The boundary conditions for $t > 0$, $\bar{z} = 0$ and $-\infty < \bar{x} < \infty$ are

$$u_{\bar{z}}(\bar{x}, 0, t) = \Delta t [H(wt - \bar{x}) - H(-\bar{x})], \tag{1.1}$$

$$\sigma_{\bar{x}\bar{z}}(\bar{x}, 0, t) = 0. \tag{1.2}$$

This problem is fairly standard and a description of the solution techniques can be found in the book by Achenbach[10]. Using Laplace transforms and the Cagniard–deHoop method for inversion of Laplace Transforms[11, 12, 10], the solution is readily found to be given as follows. Let $r = (\bar{x}^2 + \bar{z}^2)^{\frac{1}{2}}$, $\tan \theta = \bar{z}/\bar{x}$, ρ be the mass density of the material, μ and ν be the shear modulus and Poisson's ratio characterizing the material, c_L be the longitudinal wave speed and c_S be the shear wave speed. The slownesses of the longitudinal and shear waves are $a = 1/c_L$, $b = 1/c_S$ respectively and let $d = 1/w$.

Two complex variables λ and η are introduced such that

$$\lambda = -\frac{\tau}{r} \cos \bar{\theta} + i |\sin \bar{\theta}| \left(\frac{\tau^2}{r^2} - a^2 \right)^{1/2} \tag{1.3}$$
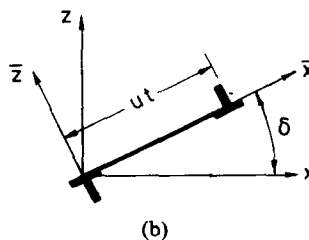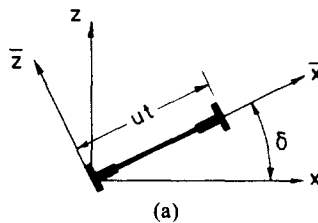

Fig. 2(a). Edge dislocation propagating out of the origin at velocity u along the $\bar{x}$-axis. (b) Shear dislocation propagating out of the origin at velocity u along the $\bar{x}$-axis.

where τ is an integration parameter and $i = (-1)^{1/2}$. η is obtained by replacing a by b in (1.3). Two complex functions α and β are introduced, defined by

$$\alpha(\lambda) = (a^2 - \lambda^2)^{1/2} \text{ and } \beta(\lambda) = (b^2 - \lambda^2)^{1/2}. \tag{1.4}$$

α is analytic in the complex λ-plane with branch cuts from $\lambda = -\infty$ to $\lambda = -a$ and $\lambda = a$ to $\lambda = \infty$. For β, the branch cuts go from $\lambda = -\infty$ to $\lambda = -b$ and $\lambda = b$ to $\lambda = \infty$.

The relevant stress components are given by

$$\Delta\sigma_{\bar{z}\bar{z}}^{E}(r/t, \bar{\theta}; w) = \Delta \int_a^{t/r} \sum_{\bar{z}\bar{z}}^{E} (r/\tau, \bar{\theta}; w) \, d(\tau/r)$$

$$= -\frac{\mu\Delta}{\pi b^2} Im \int_0^{t/r} \left\{ \frac{(2\lambda^2 - b^2)^2}{\alpha(\lambda)} \frac{2d+\lambda}{(d+\lambda)^2} \frac{\partial\lambda}{\partial(\tau/r)} H(\tau/r - a) \right.$$

$$\left. + 4\eta^2\beta(\eta) \frac{2d+\eta}{(d+\eta)^2} \frac{\partial\eta}{\partial(\tau/r)} H(\tau/r - b) \right\} d(\tau/r),$$

$$\Delta\sigma_{\bar{x}\bar{x}}^{E}(r/t, \bar{\theta}; w) = \Delta \int_a^{t/r} \sum_{\bar{x}\bar{x}}^{E} (r/t, \bar{\theta}; w) \, d(\tau/r) \tag{1.5}$$

$$= \frac{\mu\Delta}{\pi b^2} Im \int_0^{t/r} \left\{ \frac{-(b^2 - 2a^2 + 2\lambda^2)}{\alpha(\lambda)} (b - 2\lambda^2) \frac{2d+\lambda}{(d+\lambda)^2} \frac{\partial\lambda}{\partial(\tau/r)} H(\tau/r - a) \right.$$

$$\left. + 4\eta^2\beta(\eta) \frac{2d+\eta}{(d+\eta)^2} \frac{\partial\eta}{\partial(\tau/r)} H(\tau/r - b) \right\} d(\tau/r),$$

$$\Delta\sigma_{\bar{x}\bar{z}}^{E}(r/t, \bar{\theta}; w) = \Delta \int_a^{t/r} \sum_{\bar{x}\bar{z}}^{E} (r/\tau, \bar{\theta}; w) \, d(\tau/r)$$

$$= \frac{\mu\Delta}{\pi b^2} Im \int_0^{t/r} \left\{ -2\lambda(2\lambda^2 - b^2) \frac{2d+\lambda}{(d+\lambda)^2} \frac{\partial\lambda}{\partial(\tau/r)} H(\tau/r - a) \right.$$

$$\left. + 2\eta(2\eta^2 - b^2) \frac{2d+\eta}{(d+\eta)^2} \frac{\partial\eta}{\partial(\tau/r)} H(\tau/r - b) \right\} d(\tau/r),$$

where the superscript E indicates the quantity is for the edge dislocation problem. Note that these quantities are normalized for $\Delta = 1$. It is immediately observed that the stresses have the desired property of being functions of r/t and $\bar{\theta}$ only. Also, it is noted that when λ and η are real ($\bar{\theta} = 0$), in each term of the above integrals a double pole will result at d. Since these integrals must be evaluated numerically, care must be taken about these points. The method used is described in more detail in[5] and relies on separating the integrand into a regular part which is handled numerically and a singular part which is calculated analytically. This technique was also used successfully in[2].

Shear dislocation growing linearly with time

We consider a shear dislocation which appears in a linear elastic full-space at time $t = 0$ (with no crack). The geometry is the same as for the edge dislocation described above, except that the Burgers vector is a discontinuity in $u_{\bar{x}}$ and not $u_{\bar{z}}$. See Fig. 2b. Note that the problem is anti-symmetric about $\bar{z} = 0$ and therefore only the half-plane $\bar{z} > 0$ need be considered. Again zero initial conditions are used.

The boundary conditions for $t > 0$, $\bar{z} = 0$, $-\infty < \bar{x} < \infty$ are

$$u_{\bar{x}}(\bar{x}, 0, t) = \Delta t[H(wt - \bar{x}) - H(-\bar{x})], \tag{2.1}$$

$$\sigma_{\bar{z}\bar{z}}(\bar{x}, 0, t) = 0. \tag{2.2}$$

Using the notation given in the previous section, the relevant stress components are given below. A superscript S will indicate the quantity which comes from the shear dislocation

problem with $\Delta = 1$.

$$\Delta\sigma_{\bar{z}\bar{z}}^S(r/t,\bar{\theta};w) = \Delta\int_a^{t/r}\sum_{\bar{z}\bar{z}}^S(r/\tau,\bar{\theta};w)\,d(\tau/r) = \frac{\mu\Delta}{\pi b^2}\,\text{Im}\int_0^{t/r}\left\{-2\lambda(2\lambda^2-b^2)\frac{2d+\lambda}{(\lambda+d)^2}\right.$$

$$\times\frac{\partial\lambda}{\partial(\tau/r)}H(\tau/r-a)+2\eta(2\eta^2-b^2)\frac{2d+\eta}{(\eta+d)^2}\frac{\partial\eta}{\partial(\tau/r)}H(\tau/r-b)\right\}d(\tau/r),$$

$$\Delta\sigma_{\bar{x}\bar{x}}^S(r/t,\bar{\theta};w) = \Delta\int_a^{t/r}\sum_{\bar{x}\bar{x}}^S(r/\tau,\bar{\theta};w)\,d(\tau/r) = -\frac{\mu\Delta}{\pi b^2}\,\text{Im}\int_0^{t/r}\left\{2\lambda(b^2-2a^2+2\lambda^2)\right.$$

$$\times\frac{2d+\lambda}{(\lambda+d)^2}\frac{\partial\lambda}{\partial(\tau/r)}H(\tau/r-a)-2\eta(2\eta^2-b^2)$$

$$\times\frac{2d+\eta}{(\eta+d)^2}\frac{\partial\eta}{\partial(\tau/r)}H(\tau/r-b)\right\}d(\tau/r), \tag{2.3}$$

$$\Delta\sigma_{\bar{x}\bar{z}}^S(r/t,\bar{\theta};w) = \Delta\int_a^{t/r}\sum_{\bar{x}\bar{z}}^S(r/\tau,\bar{\theta};w)\,d(\tau/r) = -\frac{\mu\Delta}{\pi b^2}\,\text{Im}\int_0^{t/r}\left\{4\lambda^2\alpha(\lambda)\frac{2d+\lambda}{(\lambda+d)^2\partial(\tau/r)}\frac{\partial\lambda}{}\right.$$

$$\times H(\tau/r-a)+\frac{(2\eta^2-b^2)^2}{\beta(\eta)}\frac{2d+\eta}{(\eta+d)^2\partial(\tau/r)}\frac{\partial\eta}{}\,H(\tau/r-b)\right\}d(\tau/r).$$

Normal point load growing linearly with time

The superposition of forces applied to the old crack faces, to cancel out the stresses obtained along the old crack line due to the edge and shear dislocations, requires the solution to normal and shear point loads, which grow linearly with time and propagate out along the old crack faces at constant velocity v (no new crack). See Figs. 3(a, b).

The problem is symmetric about $z = 0$ so only the half-space $z > 0$ need be considered. Zero initial conditions are used and the boundary conditions for the normal point load are for $t > 0, z = 0$

$$\sigma_{zz}(x,0,t) = \Delta\mu t\delta(vt+x) \quad \text{for} \quad\quad x < 0, \tag{3.1}$$

$$u_z(x,0,t) = 0 \quad\quad\quad\quad \text{for } x > 0, \tag{3.2}$$

$$\sigma_{xz}(x,0,t) = 0 \quad\quad\quad\quad \text{for} -\infty < x < \infty.$$

The same solution technique is used as in the dislocation problems, except that in this case a Weiner–Hopf problem results. The method used to solve this is given in [13, 10] and since there is nothing novel about the solution, only the results will be given. Let $r = (x^2+z^2)^{1/2}$, $\tan\theta = z/x$, and λ, η be defined as in (1.3) with $\bar{\theta}$ replaced by θ. The functions α and β are decomposed into parts which are analytic in the left-hand and
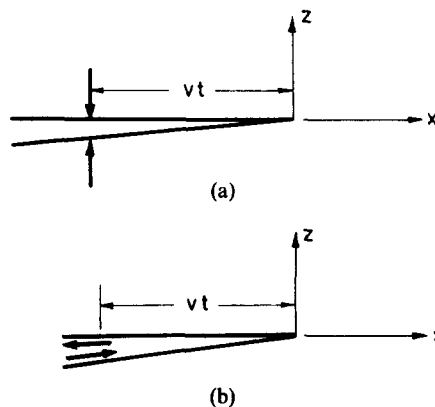

Fig. 3(a). Normal point loads propagating out along the faces of the semi-infinite crack at velocity v. (b) Shear point loads propagating out along the faces of the semi-infinite crack at velocity v.

right-hand half planes respectively. That is

$$\alpha(\lambda) = \alpha_+(\lambda)\alpha_-(\lambda) = (a + \lambda)^{1/2}(a - \lambda)^{1/2},$$

$$\beta(\lambda) = \beta_+(\lambda)\beta_-(\lambda) = (b + \lambda)^{1/2}(b - \lambda)^{1/2}, \tag{3.4}$$

where α_+, β_+ are analytic in the λ-plane with a branch cut from $\lambda = -\infty$ to $\lambda = -a, \lambda = -b$ respectively and α_-, β_- are analytic in the λ-plane with a branch cut from $\lambda = a, \lambda = b$ respectively to $\lambda = \infty$.

The Rayleigh wave function,

$$R(\lambda) = 4\lambda^2\alpha(\lambda)\beta(\lambda) + (2\lambda^2 - b^2)^2 \tag{3.5}$$

appears and must be decomposed into parts analytic in either the left- or right-hand half planes. It can be shown[10] that $R(\lambda) = 0$ has roots at $\pm 1/c$, where $1/c$ is the Rayleigh wave speed. Let $\kappa = 2(b^2 - a^2)$,

$$S_\pm = \exp\left\{-\frac{1}{\pi}\int_a^b \tan^{-1}\left[\frac{4z^2(z^2 - a^2)^{1/2}(b^2 - z^2)^{1/2}}{(b^2 - 2z^2)^2}\right]\frac{\mathrm{d}z}{z \pm \lambda}\right\} \tag{3.6}$$

and $\xi = 1/v$.

$R(\lambda)$ can be decomposed then into

$$R(\lambda) = \kappa S_+(\lambda)S_-(\lambda)(c^2 - \lambda^2). \tag{3.7}$$

The solution to the above problem is

$$\sigma_{zz}(r/t, \theta; v) = \mu\Delta\frac{\partial}{\partial v}\overset{NP}{\underset{zz}{\sum}}(r/t, \theta; v) = \frac{\mu\Delta}{\pi\kappa}\,\text{Im}\,\frac{\partial}{\partial v}\int_0^{t/r}\left\{\frac{(2\lambda^2 - b^2)^2}{\alpha_+(\lambda)}\frac{G^a(\lambda)}{S_-(\lambda)(c - \lambda)}\frac{\partial\lambda}{\partial(\tau/r)}\right.$$

$$\times H(\tau/r - a) + \frac{4\eta^2\beta(\eta)\alpha_-(\eta)}{S_-(\eta)(c - \eta)}G^a(\eta)\frac{\partial\eta}{\partial(\tau/r)}H(\tau/r - b)\bigg\}\,\mathrm{d}(\tau/r),$$

where

$$G^a(\lambda) = \frac{\alpha_+(\xi)}{S_+(\xi)(c + \xi)}\frac{1}{\lambda - \xi}, \quad \xi^2\frac{\partial(\ )}{\partial\xi} = -\frac{\partial(\ )}{\partial v},$$

$$\sigma_{xx}(r/t, \theta; v) = \mu\Delta\frac{\partial}{\partial v}\overset{NP}{\underset{xx}{\sum}}(r/t, \theta; v)$$

$$= -\frac{\mu\Delta}{\pi\kappa}\,\text{Im}\,\frac{\partial}{\partial v}\int_0^{t/r}\left\{\frac{(b^2 - 2a^2 + 2\lambda^2)(2\lambda^2 - b^2)}{\alpha_+(\lambda)S_-(\lambda)(c - \lambda)}G^a(\lambda)\frac{\partial\lambda}{\partial(\tau/r)}H(\tau/r - a)\right.$$

$$+ \frac{4\eta^2\beta(\eta)\alpha_-(\eta)}{S_-(\eta)(c - \eta)}G^a(\eta)\frac{\partial\eta}{\partial(\tau/r)}H(\tau/r - b)\bigg\}\,\mathrm{d}(\tau/r),$$

$$\sigma_{xz}(r/t, \theta; v) = \mu\Delta\frac{\partial}{\partial v}\overset{NP}{\underset{xz}{\sum}}(r/t, \theta; v) \tag{3.8}$$

$$= \frac{\mu\Delta}{\pi\kappa}\,\text{Im}\,\frac{\partial}{\partial v}\int_0^{t/r}\left\{\frac{(2\lambda^2 - b^2)2\lambda\alpha_-(\lambda)}{S_-(\lambda)(c - \lambda)}\right.$$

$$\times G^a(\lambda)\frac{\partial\lambda}{\partial(\tau/r)}H(\tau/r - a) - \frac{(2\eta^2 - b^2)2\eta}{S_-(\eta)(c - \eta)}\alpha_-(\eta)$$

$$\times G^a(\eta)\frac{\partial\eta}{\partial(\tau/r)}H(\tau/r - b)\bigg\}\,\mathrm{d}(\tau/r).$$

The superscript NP indicates the term applies to the normal point load problem.

Shear point load growing linearly with time

This problem is anti-symmetric about $z = 0$ so only the half-space need be considered. The boundary conditions for the shear point load problems are, for $t > 0, z = 0$

$$\sigma_{xz}(x, 0, t) = \mu\Delta t\delta(vt + x) \qquad\qquad x < 0, \qquad\qquad (4.1)$$

$$u_x(x, 0, t) = 0 \qquad\qquad x > 0,$$

$$\sigma_{zz}(x, 0, t) = 0 \qquad\qquad \text{for} -\infty < x < \infty.$$

The same notation as used in the normal point load problem is used. The relevant stress components are

$$\sigma_{zz}(r/t, \theta; v) = \mu\Delta\frac{\partial}{\partial v}\sum_{zz}^{SP}(r/t, \theta; v) = -\frac{\mu\Delta}{\pi\kappa}\,\text{Im}\,\frac{\partial}{\partial v}\int_0^{t/r}\left\{\frac{2\lambda\beta_-(\lambda)}{S_-(\lambda)(c-\lambda)}(2\lambda^2 - b^2)G^b(\lambda)\right.$$

$$\times\frac{\partial\lambda}{\partial(\tau/r)}H(\tau/r - a) - \frac{2\eta\beta_-(\eta)}{S_-(\eta)(c-\eta)}(2\eta^2 - b^2)G^b(\eta)\frac{\partial\eta}{\partial(\tau/r)}$$

$$\left.\times H(\tau/r - b)\right\}\,d(\tau/r),$$

where

$$G^b(\lambda) = \frac{\beta_+(\xi)}{S_+(\xi)(c+\xi)}\frac{1}{(\lambda - \xi)},\text{ and}$$

$$\sigma_{xx}(r/t, \theta; v) = \mu\Delta\frac{\partial}{\partial v}\sum_{xx}^{SP}(r/t, \theta; v) - \frac{\mu\Delta}{\pi\kappa}\,\text{Im}\,\frac{\partial}{\partial v}\int_0^{t/r}\left\{-\frac{(b^2 - 2a^2 + 2\lambda^2)}{S_-(\lambda)(c-\lambda)}2\lambda\beta_-(\lambda)G^b(\lambda)\right.$$

$$\times\frac{\partial\lambda}{\partial(\tau/r)}H(\tau/r - a) + \frac{(2\eta^2 - b^2)2\eta\beta_-(\eta)}{S_-(\eta)(c-\eta)}G^b(\eta)\frac{\partial\eta}{\partial(\tau/r)}$$

$$\left.\times H(\tau/r - b)\right\}\,d(\tau/r), \qquad\qquad (4.2)$$

$$\sigma_{xz}(r/t, \theta; v) = \mu\Delta\frac{\partial}{\partial v}\sum_{xz}^{SP}(r/t, \theta; v) = -\frac{\mu\Delta}{\pi\kappa}\,\text{Im}\,\frac{\partial}{\partial v}\int_0^{t/r}\left\{\frac{4\lambda^2\alpha(\lambda)\beta_-(\lambda)}{S_-(\lambda)(c-\lambda)}G^b(\lambda)\frac{\partial\lambda}{\partial(\tau/r)}\right.$$

$$\left.\times H(\tau/r - a) + \frac{(2\eta^2 - b^2)^2G^b(\eta)}{\beta_+(\eta)S_-(\eta)(c-\eta)\partial(\tau/r)}\frac{\partial\eta}{}H(\tau/r - b)\right\}\,d(\tau/r).$$

Superposition of point loads to cancel tractions on the old crack faces

The superposition of the above point load solutions to cancel out the tractions across the old crack line due to the two dislocations is described by Freund[14]. Since it may not be immediately obvious and is extremely useful Freund's argument will be repeated here.

We first note that it is the stresses σ_{zz} and σ_{xz} due to the dislocations which must be cancelled on the negative x-axis. From eqns (1.5) and (2.3), we observe that the stresses due to the dislocations are of the form $f(r/t)$ for $\theta = $ const. This means a fixed stress level propagates out at a constant speed $v = r/t$ along a line $\theta = $ const. Quoting from Freund[14], "In particular, a stress level $f(1/v)$ radiates out at the speed v for $t > 0$. The speed v varies between zero and the longitudinal wave speed. The x-coordinates at time t of the stress levels moving with speeds v and $v + dv$ are $-vt$ and $-(v + dv)t$, respectively. Thus, to first order terms in the infinitesimal dv, the resultant force due to all stress levels with speeds between v and $v + dv$ is $tf(1/v)\,dv$ and this force acts at $x = -vt$." Liberty has been taken in the quote to change the notation to that used in this paper.

The superposition can now be made over the range of v. The stresses due to the dislocations appearing as above, but with a semi-infinite traction free crack along the

negative x-axis are

$$\underline{\sigma}^{EC}(r/t, \theta; v) = \underline{\sigma}^{E}(r/t, \theta; u) - \int_0^{c_L} \left\{ \sigma_{zz}^{E}(v, \pi; u) \frac{\partial}{\partial v} \underline{\Sigma}^{NP}(r/t, \theta; v) \right. $$
$$\left. + \sigma_{xz}^{E}(v, \pi; u) \frac{\partial}{\partial v} \underline{\Sigma}^{SP}(r/t, \theta; v) \right\} dv \qquad (5.1)$$

where superscript EC indicates the edge dislocation appearing at the origin of a full space with a traction free semi-infinite crack along the negative x-axis. See Figs. 4(a, b). Note that the stresses due to the edge dislocation have been transformed to the x–z coordinate system. For the similar problem with the edge dislocation replaced by a shear dislocation, the stresses are as in eqn (5.1) with the superscript E's replaced by S's.

The integral in eqn (5.1) can be calculated numerically as it stands but this turns out to be extremely time consuming (on the computer). However, some observations can be made which will allow it to be integrated by parts and give an integral which will be less costly to handle. To illustrate this, consider the first part of the integral only. From (1.5) we observe $\sigma_{zz}^{E}(r/t; \theta; u)$ (obtained by rotating the coordinate system through an angle $\theta = -\delta$) depends on r/t only in the upper limit of integration. Therefore

$$\int_0^{c_L} \sigma_{zz}^{E}(v, \pi; u) \frac{\partial}{\partial v} \underline{\Sigma}^{NP}(r/t, \theta; v) dv = \int_0^{c_L} \left\{ \int_a^{1/v} \underset{zz}{\Sigma}^{E}(v; \pi; u) d\left(\frac{1}{v'}\right) \right\} \frac{\partial}{\partial v} \underline{\Sigma}^{NP}(r/t, \theta; v) dv$$

$$= \int_0^{c_L} \frac{1}{v^2} \underset{zz}{\Sigma}^{E}(v, \pi; u) \underline{\Sigma}^{NP}(r/t, \theta; v) dv + \left\{ \left[\int_a^{1/v} \underset{zz}{\Sigma}^{E}(v', \pi; u) dv' \right] \underline{\Sigma}^{NP}(r/t, \theta; u) \right\}_{v=0}^{v=c_L}. \qquad (5.2)$$

It can be shown that the term in square brackets when evaluated at $v = c_L$ and $v = 0$ is zero. Therefore, we are left with a simpler integral which is less costly to evaluate. The same manipulation can be made on the second term in the integral in eqn (5.1) and the terms coming from the shear dislocation.

FORMATION OF THE CAUCHY SINGULAR EQUATION

The dislocation solutions obtained are now superimposed over some as yet unknown distribution of dislocations using the velocity of dislocations u as the superposition parameter. Let the distribution for edge dislocations be $F^{E}(u)$ and for shear dislocations be $F^{S}(u)$. The stress at point is given by

$$\underline{\sigma}(r/t, \theta) = \int_0^{v_{CT}} \left\{ \underline{\sigma}^{EC}(r/t, \theta; u) F^{E}(u) + \underline{\sigma}^{SC}(r/t, \theta; u) F^{S}(u) \right\} du \qquad (6.1)$$
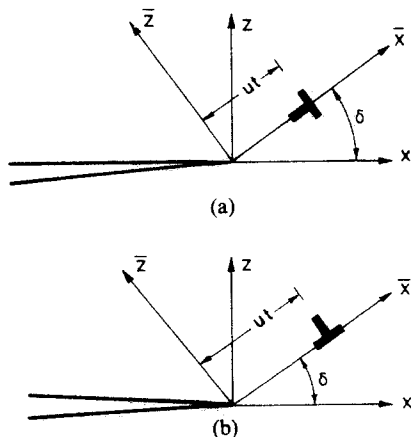

(a)

(b)

Fig. 4(a). Edge dislocation propagating out of the tip of the semi-infinite crack at velocity u along the $\bar{x}$-axis. (b) Shear dislocation propagation out of the tip of the semi-infinite crack at velocity u along the $\bar{x}$-axis.

We now note some asymptotic results for the stress field of the kinked crack. From[15], we know that the stresses near the tip of a propagating crack become infinite as the distance to the crack tip tends to zero. We also note that as $r \to 0$, the inertial effects will tend to zero; that is, the stresses will have a radial and angular dependence, the same as that of a wedge of the same angle loaded by the equivalent static tractions. From[16], for example, we can conclude that at the kink (i.e. as $r \to 0$) the stresses will be less than square root singular, (unless the loading is square root singular). This argument has been used frequently before: see for example[2, 7, 8]. We also note that for the dislocation problems with a traction free semi-infinite crack the stresses are square root singular at $r = 0$. Therefore, following[2, 7, 8], we assume the forms

$$F^E(u) = \frac{g^E(u)}{u^{1/2}(v_{CT} - u)^{1/2}}, \quad F^S(u) = \frac{g^S(u)}{u^{1/2}(v_{CT} - u)^{1/2}} \tag{6.2}$$

where $g^F(u)$ and $g^S(u)$ are bounded functions and

$$g^E(0) = g^S(0) = 0. \tag{6.3}$$

This technique has been used successfully in[2] where it could be checked with analytical results.

To solve the problems of interest, the stresses due to this super-position of dislocations along the kinked crack line is set equal to the applied stresses along this line. These applied stresses may take two forms. If the only loading is due to applied tractions on the new crack faces, the stresses are set equal to the applied stresses. If the loading is applied elsewhere (not on the new crack faces), the problem with the desired loading is first solved without the new crack. The problem with the new crack is then thought of as having the correct tractions applied to the new crack faces so that these faces do not separate. The relevant stresses due to the superposition of dislocations are then set equal to negative of the traction components applied to the new crack faces. By superposition the original problem will then be solved.

When the above procedure is performed, two coupled Cauchy singular integral equations result,

$$\sigma_{\bar{z}\bar{z}}^{\text{Loads}}(r/t, \bar{\theta} = 0) = \int_0^{v_{CT}} \left\{ \sigma_{\bar{z}\bar{z}}^{EC}(r/t, \bar{\theta}; u) F^E(u) \right.$$
$$\left. + \sigma_{\bar{z}\bar{z}}^{SC}(r/t, \bar{\theta} = 0; u) F^S(u) \right\} \mathrm{d}u \tag{6.4}$$

and

$$\sigma_{\bar{z}\bar{x}}^{\text{Loads}}(r/t, \bar{\theta} = 0) = \int_0^{v_{CT}} \left\{ \sigma_{\bar{z}\bar{x}}^{EC}(r/t, \bar{\theta} = 0; u) F^e(u) \right.$$
$$\left. + \sigma_{\bar{z}\bar{x}}^{SC}(r/t, \bar{\theta} = 0; u) F^S(u) \right\} \mathrm{d}u.$$

These equations are obviously coupled, but a procedure similar to that used in[7] can be used. For this case the Labatto–Chebyshev integration was used. If the Gauss–Chebyshev integration, together with the modification by Krenk[17], had been used, the accuracy of the results would probably be the same. As mentioned earlier, the total error is expected to be of the order of 3%.

The mode I and II stress intensity factors are given by

$$K_I = -\mu(2\pi)^{\frac{1}{2}} g^E(v_{CT}) t^{\frac{1}{2}} v_{CT}^{\frac{1}{2}} \bar{R}/b^2 (1/v_{CT}^2 - a^2)^{-\frac{1}{2}}, \tag{6.5}$$

$$K_{II} = -\mu(2\pi)^{\frac{1}{2}} g^S(v_{CT}) t^{\frac{1}{2}} v^{\frac{1}{2}}_{CT} \bar{R}/b^2 (1/v_{CT}^2 - b^2)^{-\frac{1}{2}},$$

where

$$\bar{R} = (2/v_{CT}^2 - b^2)^2 + 4/v_{CT}^2(a^2 - 1/v_{CT}^2)^{\frac{1}{2}}(b^2 - 1/v_{CT}^2)^{\frac{1}{2}}. \tag{6.6}$$

LOADING CASES

In each case, two loadings will be considered.

Case (a)

The first loading will be constant normal tractions with zero shear tractions applied to the new crack faces. The second will be constant shear tractions with zero normal tractions applied to the new crack faces. For the first loading, the results show that K_{II} is negligible and for the second K_I is negligible. By negligible it is means at least one to two orders of magnitude less than the other stress intensity factor. In eqn (6.4),

$$\sigma_{\bar{z}\bar{z}}^{\text{Loads}}(r/t, \bar{\theta} = 0) = \mu\Delta, \quad \sigma_{\bar{z}\bar{x}}^{\text{Loads}}(r/t, \bar{\theta} = 0) = 0 \tag{7.1}$$

for the first loading and

$$\sigma_{\bar{z}\bar{z}}^{\text{Loads}}(r/t, \bar{\theta} = 0) = 0, \quad \sigma_{\bar{z}\bar{x}}^{\text{Loads}}(r/t, \bar{\theta} = 0) = \mu\Delta \tag{7.2}$$

for the second loading.

Case (b)

The first loading is constant normal tractions with zero shear tractions applied to the old crack faces at time $t = 0$ and the second loading is constant shear tractions with zero normal tractions applied to the old crack faces at time $t = 0$. The expressions will be given later as special cases of the loadings in case (c).

Case (c)

The effect of a planar stress wave impinging on the old crack is modeled here. Let the axis parallel and perpendicular to the wave front be denoted by as shown in Fig. 1. The x'-axis makes an angle α with the x-axis.

This first case corresponds to a jump in the strain component $\epsilon_{z'z'}$ from zero ahead of the stress wave to a constant value $\mu\Delta_N$ behind the wavefront before the stress wave meets the old crack. The value of the other strain components is zero. The problem of this stress wave meeting the old crack, with no kink forming, can be solved by superposition. It can be split up into two problems; the first is a planar stress wave propagating through an infinite body (no crack present) and the second is an infinite body with a semi-infinite crack (which is the old crack), with just the correct tractions applied to the crack faces such that the sum of two problems gives zero tractions on the old crack. The boundary conditions for the second problem, on the old crack faces, are for $t > 0, z = 0, x < 0$

$$\sigma_{zz}(x, 0, t) = -(1 - 2a^2/b^2 \sin^2 \alpha)\mu\Delta_N H(c_L t + \sin \alpha x),$$

$$\sigma_{xz}(x, 0, t) = 2a^2/b^2 \cos \alpha \sin \alpha \mu\Delta_N H(c_L + \sin \alpha x). \tag{7.3}$$

The initial conditions are zero at $t = 0$.

This problem can again be separated into two parts, which are either symmetric or antisymmetric about $z = 0$. Therefore, only the half-space $z > 0$ need be considered. We first note that the intersection of the wave front and the negative x-axis is a point moving at a speed $v_L = c_L/\sin \alpha$. Two parts are then (1) the case when on $z = 0, t > 0$

$$\sigma_{zz}(x, 0, t) = \mu\Delta_N H(t + x/v_L) \qquad \text{for } x < 0,$$

$$\sigma_{xz}(x, 0, t) = 0 \qquad \text{for } x < 0, \tag{7.4}$$

and

$$u_z(x, 0, t) = 0 \qquad\qquad \text{for } x > 0.$$

with zero initial conditions, and (2) the case when on $z = 0$, $t > 0$,

$$\sigma_{zz}(x, 0, t) = 0 \qquad\qquad \text{for } x < 0,$$

$$\sigma_{xz}(x, 0, t) = \mu \Delta_N H(t + x/v_L) \qquad \text{for } x < 0, \tag{7.5}$$

and

$$u_x(x, 0, t) = 0 \qquad\qquad \text{for } x > 0.$$

The solution to the first and second parts is just

$$\mu \Delta_N \sum^{NP} (r/t, \theta; v_L) \quad \text{and} \quad \mu \Delta_N \sum^{SP} (r/t, \theta; v_L)$$

respectively. Therefore, the solution to the superposition problem with the crack for the first case with boundary conditions, given by (7.3) is given by

$$\begin{aligned}
\underline{\sigma}(r/t, \theta &= -(1 - 2a^2/b^2 \sin^2 \alpha)\mu \Delta_N \sum^{NP} (r/t, \theta; v_L) \\
&+ 2a^2/b^2 \cos \alpha \sin \alpha \mu \Delta_N \sum^{SP} (r/t, \theta; v_L).
\end{aligned} \tag{7.6}$$

For the stresses of the first case of loading case (c), the stresses due to the plane stress wave in an infinite body (no crack) must be added; that is, the stresses

$$\begin{aligned}
\sigma_{z'z'}(x', z', t) &= \mu \Delta_N H(c_L t - z'), \\
\sigma_{x'x'}(x', z', t) &= (1 - 2a^2/b^2)\mu \Delta_N(c_L t - z'), \\
\sigma_{x'z'}(x', z', t) &= 0
\end{aligned} \tag{7.7}$$

must be added to the stresses in eqn (7.6).

For the second case, the stress wave represents a jump in the strain component $\epsilon_{z'x'}$ from zero ahead of the planar wave front to a constant $\mu \Delta_S$, behind the wave front before meeting the crack-tip. Again the problem can be split up into a problem with no new crack and a problem with the new crack. The boundary conditions on the old crack faces for the latter problem are for $t > 0$, $z = 0$, $x < 0$

$$\begin{aligned}
\sigma_{zz}(x, 0, t) &= -2 \cos \alpha \sin \alpha \mu \Delta_S H(c_S t + \sin \alpha x), \\
\sigma_{xz}(x, 0, t) &= -(\cos \alpha^2 - \sin^2 \alpha)\mu \Delta_S H(c_S t + \sin \alpha x).
\end{aligned} \tag{7.8}$$

with zero initial conditions. Again, this can be split into two problems for which the solution is known. Let $v_S = c_S/\sin \alpha$. The solution to the problem with the crack with boundary conditions given by eqn (7.8) is

$$\begin{aligned}
\underline{\sigma}(r/t, \theta) &= -2 \cos \alpha \sin \alpha \mu \Delta_S \sum^{NP} (r/t, \theta; v_S) \\
&- (\cos^2 \alpha - \sin^2 \alpha)\mu \Delta_S \sum^{SP} (r/t, \theta; v_S).
\end{aligned} \tag{7.9}$$

The stresses for the second part of loading case (c) are then given by adding

$$\begin{aligned}
\sigma_{z'z'}(x', z', t) &= 0, \sigma_{z'x'}(x', z', t) = 0 \\
\sigma_{x'z'}(x', z', t) &= \mu \Delta_S H(c_S t - z')
\end{aligned} \tag{7.10}$$

to the stresses in (7.9).

Note that the two cases in loading case (b) can be obtained by setting $x = 0$ and $v_L = v_S = 0$ in eqns (7.6) and (7.9).

NUMERICAL PROCEDURE

The superposition calculation to obtain $\underline{\sigma}^{EC}$ and $\underline{\sigma}^{SC}$ and the evaluation of Σ^{NP} and Σ^{SP} is done numerically. Gaussian integration was used with the algorithms given in[18]. The integration ranges were split up as follows: if $r/t < 0.1 \, c_S$, the integral was split up into three ranges; the first from r/t to $r/t + 0.1 \, c_S$; the second from $r/t + 0.1 \, c_S$ to c_S and the third from c_S to c_L. Otherwise, if $r/t > 0.1 \, c_S$, only two ranges were used: the first from r/t to c_S and the second from c_S to c_L. In each range 25 integration points were used.

Only when $\theta \to \pi/2$ and/or when $r/t \to 0$ was there any problem with the numerical integration. If too many integration points were chosen when r/t was close to 0, a numerical instability occurred. This was due to the integrands being the difference in two functions, both of which are very large as $r/t \to 0$. With 25 integration points and 11 collocation points in the solution of the integral equations, this problem was avoided and still gave sufficiently accurate results.

A problem occurred in the evaluation of Σ^{NP} and Σ^{SP} when $v \to 0$ and $\theta \to \pi/2$. There is a pole on the real λ-axis in the integrand for these two functions and as $\theta \to \pi/2$ with v small, this affected the integration. Satisfactory covergence was obtained up to $\theta = 0.485 \, \pi$. To obtain results at $\theta = \pi/2$, the results were extrapolated from those for $\theta < 0.485 \, \pi$.

RESULTS AND DISCUSSION

For loading case (a) the results for K_I and K_{II} are presented in Fig. 5. Note that for all results a Poisson's ratio of $1/4$ was used which gives a ratio of wave speeds $c_s = c_L/3^{\frac{1}{2}}$, $c_R = c_L/(3.549)^{\frac{1}{2}}$. K_{II} for normal loading and K_I for shear loading are less than 2% of the other stress intensity factor for the same loading and $\delta/\pi \leq 0.25$. At $\delta/\pi = 0.5$ they are still less than 15%, which means they are essentially insignificant when compared to the stress intensity factor corresponding to the mode of loading at the crack tip. This implies that for finite loads on the new crack faces the geometry of the corner has only a minor effect on the stress intensity factor at the kinked crack tip.

An interesting comparison can be made with Freund's result in[13] for the case $\delta = 0$ and time independent loading. This result shows that for $\delta = 0$

$$K_\alpha(l = v_{CT}t, \, t) = k_\alpha(v_{CT})K_S(l = v_{CT}t), \tag{8.1}$$

where $\alpha = I$ or II for normal or shear loading, $k_\alpha(v_{CT})$ is a universal function of instantaneous crack tip velocity and K_S is the static stress intensity factor for a crack that has its length increased, by an amount $l = v_{CT}t$ under the same time independent loading. $k_\alpha(v_{CT})$ is given in[13] for mode I and in[19] for mode II. (Note that Fig. 2 in[13] is slightly in error.) K_S can be eliminated by comparing two cracks propagating with velocities v_1, v_2 such that $v_1 t_1 = v_2 t_2$. Then

$$\frac{K_\alpha(l = v_1 t_1, \, t_1)}{K_\alpha(l = v_2 t_2, \, t_2)} = \frac{k_\alpha(v_1)}{k_\alpha(v_2)}. \tag{8.2}$$

If the left hand side is calculated from the results presented herein, choosing $v_2 = 0.1 \, c_R$ and comparing the results for the different values of δ, we find that for $\delta \leq 0.25 \, \pi$ the results are within 5% of Freund's results and even up to $\delta = 0.5 \, \pi$ the results are within 11%. It seems possible then that at least for the time independent loading case such as case (a) that the results could be phrased as in eqn (8.1) with the same function $k_\alpha(v_{CT})$.

For loading case (b), the results for normal and shear loading are given in Fig. 6(a, b). For normal loading, K_I decreases with δ, with the amount of decrease decreasing with c_{CT} increasing until for $v_{CT} = 0.9 \, c_R$, K_I increases with δ slightly. For the shear loading the decrease in K_{II} with δ is not as dramatic. However, in both cases the other stress intensity factor (K_{II} for normal loading, K_I for shear loading) increases rapidly (almost linearly with δ) except for $v_{CT} = 0.9 \, c_R$. For the normal loading case, there will be a velocity between $0.7 \, c_R$ and $0.9 \, c_R$ which will have $K_{II} = 0$ for some δ in the range 0 to $\pi/2$. A suggested model for
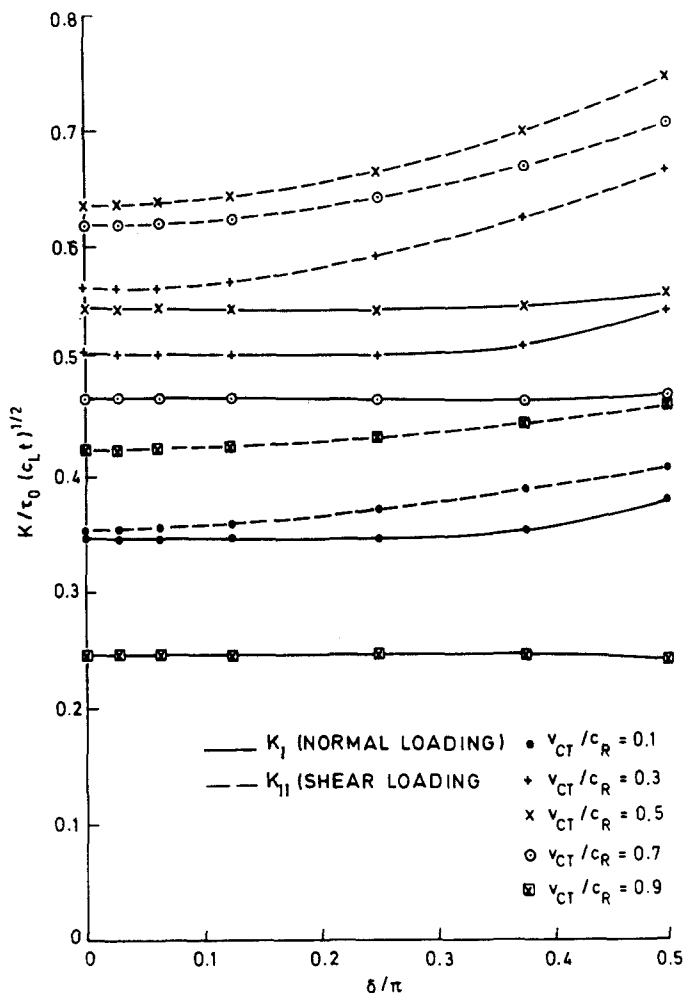
Fig. 5. K_I for constant normal loading and K_{II} for constant shear loading on the new crack faces with $\tau_0 = \mu\Delta$.

quasistatic crack kinking is that the crack will propagate so that $K_{II} = 0$[20]. If this was so, and the crack would initiate as modeled herein, then it will do so for this loading with $\delta > 0$ at a higher velocity than normally observed for crack propagation. For shear loading, the increase in K_I with δ may have application to geophysical fault modeling. In this case if fracture occurs predominantly in mode I the conclusion would be for the crack to initiate again at a high velocity.

It must be pointed out that requiring the solutions to be self-similar in r/t prevents a delay time for crack initiation after the instant of load application being included in the above results. However, Freund has extended his result to show that for the case $\delta = 0$, the instantaneous stress intensity factor does not depend on delay time provided times greater than the delay time are considered[14]. From the close correlation between Freund's result for the time independent loading case with $\delta = 0$, and the case when $\delta \neq 0$ as calculated above, it may be true that delay times for $\delta \neq 0$ can be treated as for the case $\delta = 0$. This cannot be proven here but it does not appear to be an unreasonable expectation.

If the stresses used for $\sigma_{\hat{z}\hat{z}}^{\text{Loads}}$ and $\sigma_{\hat{x}\hat{z}}^{\text{Loads}}$ are considered, they are seen to follow the trends of K_I, K_{II} with respect to dependence on $\delta, r/t$. Although this is not entirely unexpected, it has not been exploited before. This may be because nowhere in the literature could plots of stress versus r/t for different values of θ be found for the dynamic stress field around a crack.

The stress intensity factors for case (c) are given for a number of angles α and δ in Tables 1(a)–2(d) where the values for K_I and K_{II} are normalized by $\mu\Delta(c_L t)^{\frac{1}{2}}$. Firstly, when
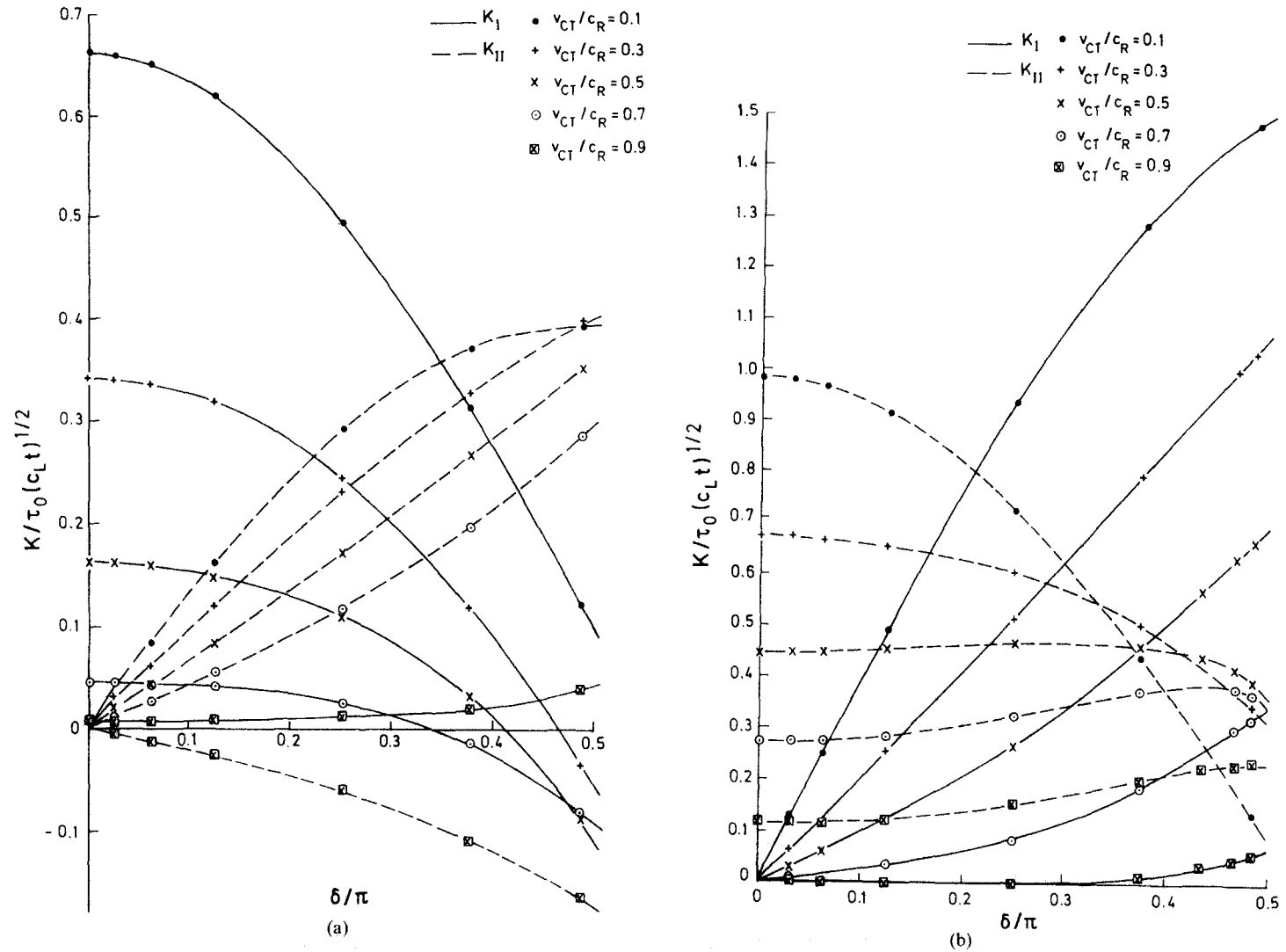
Fig. 6(a). Stress intensity factors for normal step function loading on the old crack faces with $\tau_0 = \mu\Delta$. (b) Stress intensity factors for shear step function loading on the old crack faces with $\tau_0 = \mu\Delta$.

Table 1(a). Normal stress wave loading at angle α with kinked crack propagating at $v_{CT}/c_R = 0.1$

α/π	δ/π	0	.0625	.125	.25	.375	.485
0	K_I	1.0070	.9870	.9291	.7241	.4625	.2482
	K_{II}	0	.1287	.2465	.4131	.4564	.3952
.03125	K_I	.9831	.9875	.9531	.7864	.5452	.3327
	K_{II}	-.0838	.0449	.1680	.3587	.4353	.4022
.0625	K_I	.9483	.9752	.9633	.8357	.6180	.4115
	K_{II}	-.1590	-.0333	.0921	.3014	.4081	.4026
.125	K_I	.8514	.9154	.9436	.8927	.7297	.5441
	K_{II}	-.2775	-.1656	-.0446	.1842	.3392	.3845
.25	K_I	.5992	.6968	.7734	.8440	.7970	.6796
	K_{II}	-.3614	-.2995	-.2170	-.0178	.1734	.2881
.375	K_I	.3761	.4486	.5189	.6277	.6614	.6178
	K_{II}	-.2439	-.2364	-.2104	-.1069	.0375	.1584
.45	K_I	.3027	.3380	.3797	.4628	.5095	.4936
	K_{II}	-.1056	-.1197	-.1228	-.0864	.0005	.0930
.485	K_I	.2894	.3041	.3278	.3872	.4291	.4241
	K_{II}	-.0320	-.0521	-.0653	-.0579	-.00175	.0751

Table 1(b). Normal stress wave loading at angle α with kinked crack propagating at $v_{CT}/c_R = 0.3$

α/π	δ/π	0	.0625	.125	.25	.375	.485
0	K_I	.8484	.8295	.7747	.5818	.3387	.1435
	K_{II}	0	.1342	.2564	.4260	.4636	.3962
.03125	K_I	.8362	.8342	.7989	.6359	.4050	.2055
	K_{II}	-.0778	.0565	.1846	.3795	.4499	.4073
.0625	K_I	.8071	.8281	.8123	.6816	.4672	.2680
	K_{II}	-.1484	-.0175	.1129	.3276	.4288	.4118
.125	K_I	.7315	.7858	.8066	.7451	.5749	.3868
	K_{II}	-.2614	-.1475	-.0229	.2131	.3664	.4007
.25	K_I	.5228	.6110	.6828	.7491	.6957	.5678
	K_{II}	-.3457	-.2945	-.2174	-.0146	.1874	.3060
.375	K_I	.3314	.4012	.4763	.6075	.6608	.6197
	K_{II}	-.2356	-.2534	-.2461	-.1540	.0092	.1569
.45	K_I	.2674	.3049	.3582	.4817	.5697	.5744
	K_{II}	-.1020	-.1476	-.1762	-.1625	-.0572	.0736
.485	K_I	.2558	.2749	.3129	.4206	.5137	.5344
	K_{II}	-.0310	-.0837	-.1247	-.1449	-.0717	.0429

Table 1(c). Normal stress wave loading at angle α with kinked crack propagating at $v_{CT}/c_R = 0.5$

α/π	δ/π	0	.0625	.125	.25	.375	.485
0	K_I	.7078	.6911	.6427	.4744	.2674	.1068
	K_{II}	0	.1245	.2373	.3909	.4202	.3551
.03125	K_I	.6982	.6987	.6665	.5212	.3200	.1515
	K_{II}	-.0685	.0563	.1752	.3539	.4140	.3703
.0625	K_I	.6801	.6973	.6817	.5625	.3716	.1990
	K_{II}	-.1313	-.0098	.1117	.3106	.4005	.3797
.125	K_I	.6218	.6685	.6854	.6255	.4674	.2964
	K_{II}	-.2333	-.1289	-.0127	.2095	.3521	.3800
.25	K_I	.4506	.5294	.5949	.6552	.6002	.4735
	K_{II}	-.3130	-.2725	-.2039	-.0105	.1884	.3049
.375	K_I	.2880	.3526	.4257	.5579	.6131	.5702
	K_{II}	-.2151	-.2461	-.2491	-.1665	.0013	.1586
.45	K_I	.2330	.2693	.3247	.4589	.5581	.5668
	K_{II}	-.0933	-.1534	-.1940	-.1923	-.0807	.0672
.485	K_I	.2230	.2430	.2854	.4088	.5189	.5478
	K_{II}	-.0284	-.0959	-.1496	-.1833	-.1034	.0308

P. BURGERS

Table 1(d). Normal stress wave loading at angle α with kinked crack propagating at $v_{CT}/c_R = 0.7$

α/π	δ/π	0	.0625	.125	.25	.375	.485
0	K_I	.5139	.5011	.4644	.3385	.1895	.0805
	K_{II}	0	.1069	.2031	.3301	.3479	.2890
.03125	K_I	.5095	.5094	.4844	.3738	.2859	.1080
	K_{II}	-.0568	.0506	.1526	.3030	.3477	.3057
.0625	K_I	.4986	.5111	.4984	.4062	.2629	.1389
	K_{II}	-.1093	-.0049	.0999	.2695	.3412	.3181
.125	K_I	.4597	.4949	.5071	.4586	.3355	.2065
	K_{II}	-.1959	-.1067	-.0060	.1873	.3084	.3278
.25	K_I	.3373	.3986	.4499	.4967	.4500	.3463
	K_{II}	-.2659	-.2355	-.1777	-.0056	.1740	.2781
.375	K_I	.2172	.2684	.3281	.4379	.4834	.4456
	K_{II}	-.1841	-.2199	-.2281	-.1566	.0006	.1505
.45	K_I	.1760	.2057	.2527	.3688	.4557	.4639
	K_{II}	-.0800	-.1429	-.1866	-.1909	-.0838	.0619
.485	K_I	.1685	.1856	.2228	.3325	.4317	.4594
	K_{II}	-.0243	-.0935	-.1505	-.1885	-.1109	.0243

Table 2(a). Shear stress wave loading at angle α with kinked crack propagating at $v_{CT}/c_R = 0.1$

α/π	δ/π	0	.0625	.125	.25	.375	.485
0	K_I	0	-.3814	-.7365	-1.2803	-1.5241	-1.4983
	K_{II}	1.3369	1.2940	1.1695	.7321	.1837	-.2586
.03125	K_I	.1906	-.1693	-.5178	-1.0880	-1.3900	-1.4180
	K_{II}	1.2329	1.2350	1.1564	.7958	.2866	-.1460
.0625	K_I	.3637	.0336	-.3000	-.8823	-1.2343	-1.3146
	K_{II}	1.1018	1.1475	1.1153	.8386	.3796	-.0436
.125	K_I	.6396	.3908	.1107	-.4505	-.8718	-1.0558
	K_{II}	.7746	.8973	.9541	.8553	.5247	.1487
.25	K_I	.8407	.8054	.7038	.3551	-.0539	-.3353
	K_{II}	0	.2048	.3873	.6135	.6000	.4153
.375	K_I	.5700	.7357	.8394	.8489	.6495	.4078
	K_{II}	-.6514	-.4853	-.2901	.1015	.3697	.4402
.45	K_I	.2462	.4878	.6882	.9156	.9015	.7518
	K_{II}	-.8623	-.7687	-.6224	-.2414	.1244	.3323
.485	K_I	.0749	.3349	.5670	.8825	.9581	.8645
	K_{II}	-.9002	-.8483	-.7362	-.3884	-.0027	.2561

Table 2(b). Shear stress wave loading at angle α with kinked crack propagating at $v_{CT}/c_R = 0.3$

α/π	δ/π	0	.0625	.125	.25	.375	.485
0	K_I	0	-.3179	-.6086	-1.0231	-1.1571	-1.0589
	K_{II}	1.2351	1.1897	1.0590	.6119	.0871	-.2986
.03125	K_I	.1621	-.1447	-.4410	-.9045	-1.1028	-1.0616
	K_{II}	1.1491	1.1593	1.0812	.7105	.2077	-.1833
.0625	K_I	.3118	.0242	-.2697	-.7706	-1.0356	-1.0489
	K_{II}	1.0356	1.1001	1.0762	.7917	.3239	-.0781
.125	K_I	.5569	.3302	.0654	-.4688	-.8479	-.9723
	K_{II}	.7394	.9008	.9827	.8895	.5284	.1335
.25	K_I	.7504	.7077	.5849	.1686	-.3048	-.6106
	K_{II}	0	.2668	.5024	.7820	.7376	.4801
.375	K_I	.5166	.6640	.7357	.6391	.3037	-.0401
	K_{II}	.6471	-.4303	-.1794	.3027	.5820	.5812
.45	K_I	.2241	.4477	.6204	.7512	.5956	.3216
	K_{II}	-.8602	-.7384	-.5508	-.0799	.3241	.4850
.485	K_I	.0682	.3116	.5198	.7503	.6934	.4739
	K_{II}	-.8987	-.8315	-.6884	-.2584	.1752	.4202

Table 2(c). Shear stress wave loading at angle α with kinked crack propagating at $v_{CT}/c_R = 0.5$

α/π	δ/π	0	.0625	.125	.25	.375	.485
0	K_I	0	-.2648	-.5021	-.8104	-.8479	-.7102
	K_{II}	1.0823	1.0369	.9070	.4725	-.0095	-.3290
.03125	K_I	.1364	-.1242	-.3732	-.7385	-.8435	-.7453
	K_{II}	1.0157	1.0269	.9485	.5812	.1058	-.2329
.0625	K_I	.2645	.0159	-.2375	-.6504	-.8235	-.7715
	K_{II}	.9228	.9895	.9651	.6769	.2221	-.1406
.125	K_I	.4791	.2770	.0384	-.4334	-.7340	-.7876
	K_{II}	.6682	.8352	.9180	.8142	.4429	.0617
.25	K_I	.6591	.6162	.4935	.0827	-.3674	-.6332
	K_{II}	0	.2783	.5224	.8014	.7318	.4456
.375	K_I	.4591	.5913	.6462	.5108	.1369	-.2282
	K_{II}	-.6041	-.3750	-.1111	.3931	.6669	.6314
.45	K_I	.1998	.4042	.5554	.6331	.4123	.0827
	K_{II}	-.8056	-.6763	-.4753	.0268	.4427	.5791
.485	K_I	.0608	.2843	.4705	.6447	.5145	.2272
	K_{II}	-.8421	-.7699	-.6148	-.1518	.3009	.5099

Table 2(d). Shear stress wave loading at angle α with kinked crack propagating at $v_{CT}/c_R = 0.7$

α/π	δ/π	0	.0625	.125	.25	.375	.485
0	K_I	0	-.1938	-.3622	-.5558	-.5248	-.3790
	K_{II}	.8920	.8493	.7278	.3297	-.0844	-.3199
.03125	K_I	.0997	-.0937	-.2761	-.5221	-.5452	-.4216
	K_{II}	.8443	.8535	.7780	.4340	.0124	-.2548
.0675	K_I	.1951	.0077	-.1820	-.4739	-.5544	-.4613
	K_{II}	.7729	.8333	.8066	.5298	.1148	-.1859
.125	K_I	.3581	.2019	.0169	-.3382	-.5328	-.5207
	K_{II}	.5669	.7203	.7924	.6795	.3226	-.0202
.25	K_I	.5014	.4659	.3645	.0299	-.3211	-.5028
	K_{II}	0	.2585	.4836	.7298	.6399	.3535
.375	K_I	.3526	.4559	.4942	.3653	.0415	-.2621
	K_{II}	-.5265	-.3128	-.0634	.4083	.6516	.5947
.45	K_I	.1539	.3153	.4315	.4714	.2574	-.0412
	K_{II}	-.7040	-.5816	-.3896	.0901	.4795	.5911
.485	K_I	.0468	.2239	.3688	.4867	.3418	.0682
	K_{II}	-.7362	-.6669	-.5170	-.0701	.3601	.5444

$K_I < 0$ the boundary conditions assumed are violated in that this implies interpretation of the cracked kinked faces. Since $K_I < 0$ does not imply any physically reasonable condition for this analysis and the assumed boundary conditions are violated the signs of the loading must be changed in these situations for the results to have any meaning. For both normal and shear stress wave loading $K_\alpha(\alpha = I$ for normal, II for shear) has a maximum close to $\alpha = \delta$. Also the other stress intensity factor is close to zero at this point. This latter condition may be the appropriate criterion for choosing a particular kinking angle δ for a particular α. For those cases of shear loading when $K_I < 0$, the problem would have to be resolved allowing for contact between the crack faces if the solution for that particular loading was required.

It is tempting to use the maximum value of energy release rate G [15] with respect to δ for a particular v_{CT} and α as a criterion for choosing δ and v_{CT}. Since G is proportional to t this seems to be an unreasonable approach (although no more unreasonable than using critical stress intensity factor as a criterion) for the above model. This is not meant to imply that the criterion is incorrect. More likely the model that has been used is at fault.

Before a criterion for kinking can be developed, more experimental results must be available. As mentioned already, the results coming out of[1] will help, but the conditions immediately after kinking must be quantitatively determined.

REFERENCES

1. K. Ravi Chander and W. G. Knauss, Experiments in dynamic crack propagation. *Pres. S.E.S. 18th Ann. Meeting*, 2–4 Sept 1981 at Brown University, Rhode Island, U.S.A.
2. P. Burgers, Dynamic propagation of a kinked or bifurcated crack in anti-plane strain. *J. Appl. Mech.* **49**, 371–376 (1982).
3. P. Burgers and J. P. Dempsey, Two analytical solutions for dynamic crack bifurcation in anti-plane strain. *J. Appl. Mech.* **49**, 366–370 (1982).
4. J. Aboudi, The dynamic stresses induced by the propagation of skew cracks. *Com. Meth. Appl. Mech. and Engng* **15**, 181–199 (1978).
5. P. Burgers and L. B. Freund, An addendum to the paper: dynamic growth of an edge crack in a half space. *Int. J. Solids Structures* **17**, 721–727 (1981).
6. J. R. Rice, Mathematical analysis in the mechanics of fracture. *Fracture* (Edited by H. Liebowitz), Vol. 2, pp. 191–311. Academic Press, New York (1968).
7. K. K. Lo, Analysis of branched cracks. *J. Appl. Mech.* **45**, 797–802 (1978).
8. N. I. Ioakimidis and P. S. Theocaris, The modified Lobatto–Chebyshev method applied to the numerical evaluation of stress intensity factors in cracks with a corner point. *Rev. Roum. Sci. Techn. -Mec. Appl.* **25**, 151–159 (1980).
9. F. Erdogan and G. D. Gupta, On the numerical solution of singular integral equations. *Mechanics of Fracture* (Edited by G. C. Sih), pp. 368–425. Noordhoff, Leyden, Netherlands (1973).
10. J. D. Achenbach, *Wave Propagation in Elastic Solids*. North-Holland, Amsterdam (1975).
11. A. T. DeHoop, A modification of Cagniard's method for solving seismic pulse problems. *Appl. Sci. Res.* 349–356 (1961).
12. L. B. Freund, Course notes from '*Stress Waves in Solids*' offered in 1975, Brown University, Providence.
13. L. B. Freund, Crack propagation in an elastic solid subjected to general loading—I. Constant rate of extension. *J. Mech. Phys. Solids* **20**, 129–140 (1972).
14. L. B. Freund, Crack propagation in an elastic solid subjected to general loading—II. Non-uniform rate of extension. *J. Mech. Phys. Solids* **20**, 141–152 (1972).
15. L. B. Freund and R. J. Clifton, On the uniqueness of elastodynamic solutions for running cracks. *J. Elasticity* **4**, 293–299 (1974).
16. J. P. Dempsey, The wedge subjected to tractions: a paradox resolved. *J. Elasticity* **11**, 1–10 (1981).
17. S. Krenk, On the use of the interpolation polynomial solutions of singular integral equations. *Quart. Appl. Math.* 479–484 (1975).
18. A. H. Stroud and D. Secrest, *Gaussian Quadrature Formulas*. Prentice-Hall, Englewood Cliffs, New Jersey.
19. A. F. Fossum and L. B. Freund, Nonuniformly moving shear crack model of a shallow focus earthquake mechanism. *J. Geophys. Res.* **80**, 367–385 (1975).
20. B. Cotterell and J. R. Rice, Slightly curved or kinked cracks. *Int. J. Fracture* **16**, 155–169 (1980).